Detection of Cl^- Binding to Band 3 by Double-Quantum-Filtered ^{35}Cl Nuclear Magnetic Resonance

D. Liu, P. A. Knauf, and S. D. Kennedy
Department of Biophysics, University of Rochester, Rochester, New York 14642 USA

ABSTRACT We have applied double-quantum-filtered (DQF) NMR of ^{35}Cl to study binding of Cl^- to external sites on intact red blood cells, including the outward-facing anion transport sites of band 3, an integral membrane protein. A DQF ^{35}Cl NMR signal was observed in cell suspensions containing 150 mM KCl, but the DQF signal can be totally eliminated by adding 500 μM 4,4′-dinitrostilbene-2,2′-disulfonate (DNDS), an inhibitor that interferes with Cl^- binding to the band 3 transport site. Therefore, it seems that only the binding of Cl^- to transport sites of band 3 can give rise to a ^{35}Cl DQF signal from red blood cell suspensions. In accordance with this concept, analysis of the single quantum free induction decay (FID) revealed that signals from buffer and DNDS-treated cells were fitted with a single exponential function, whereas the FID signals of untreated control cells were biexponential. The DQF signal remained after the cells were treated with eosin-5-maleimide (EM), a noncompetitive inhibitor of chloride exchange. This result supports previous reports that EM does not block the external chloride binding site. The band 3-dependent DQF signal is shown to be caused at least in part by nonisotropic motions of Cl^- in the transport site, resulting in incompletely averaged quadrupolar couplings.

INTRODUCTION

^{35}Cl NMR linewidth measurements have long been applied in the study of interactions between chloride ions and proteins (Forsen and Lindman, 1981). Band 3 is an anion exchange protein found in the membrane of human red blood cells, and the binding of Cl^- to band 3 has been extensively studied by ^{35}Cl NMR (Falke et al., 1984a,b, 1985a,b; Price et al., 1991; Minami et al., 1992; Glibowicka et al., 1988; Galanter and Labotka, 1991; Falke and Chan, 1985, 1986a,b,c). By analyzing ^{35}Cl line broadening, Falke et al. (1984b) have shown that there are two kinds of Cl^- binding sites on the surface of red cells. The broadening due to one kind of site is saturable and can be eliminated by adding DNDS, which, although it is not a strictly competitive inhibitor (Aranibar et al., 1994; Knauf et al., 1993a), strongly interferes with binding of chloride to the band 3 transport site (Fröhlich, 1982). Further evidence that these "high-affinity" sites represent the Cl^- transport sites is provided by the fact that their affinities as measured by NMR agree with the transport site affinity from Cl^- flux experiments (Falke et al., 1984b). The DNDS-insensitive sites have a very low affinity for Cl^- and, accordingly, the DNDS-insensitive line broadening is nearly equal to the nonsaturable (low-affinity) component of ^{35}Cl line broadening (Liu et al., 1995; Falke et al., 1984b). These low-affinity sites do not seem to be related to the transport sites. Thus, DNDS sensitivity can be used operationally to distinguish transport sites from nonspecific Cl^- binding sites.

^{35}Cl belongs to a class of nuclei with spin quantum number 3/2 and a large electrical quadrupole moment. Although the spin 3/2 system has three single quantum transitions ($+\frac{1}{2} \leftrightarrow -\frac{1}{2}$; $+\frac{3}{2} \leftrightarrow +\frac{1}{2}$; $-\frac{3}{2} \leftrightarrow -\frac{1}{2}$), rapid isotropic motion of the quadrupolar ion in aqueous solution causes the relaxation rate and energy of the three transitions to be equal. In this case, the central ($+\frac{1}{2} \leftrightarrow -\frac{1}{2}$) and satellite ($+\frac{3}{2} \leftrightarrow +\frac{1}{2}$ and $-\frac{3}{2} \leftrightarrow -\frac{1}{2}$) transitions have equivalent properties and the NMR signal decays exponentially. When the ion binds to a macromolecule, there is usually an increase in the rate of transverse magnetization decay, or, equivalently, an increase of the spectral linewidth. In addition, the central and satellite transitions may no longer have identical relaxation properties, resulting in nonexponential magnetization decay (Hubbard, 1969, 1970; Bull, 1972).

Most previous ^{35}Cl NMR experiments with band 3 (and other proteins) were analyzed by using a Lorentzian function to describe the spectral lineshapes. We have observed that, in a 9.4 Tesla magnetic field, the ^{35}Cl free induction decay (FID) signal from extracellular Cl^- in intact red blood cell suspensions is not an exponentially decaying signal, resulting in a non-Lorentzian lineshape. The data are better fitted with a biexponential function. Price et al. have also observed nonexponential magnetization decay in erythrocyte ghosts (Price et al., 1991).

These findings led us to perform double-quantum-filtered (DQF) NMR experiments on the system. Double- and triple-quantum-filtered NMR of ^{23}Na has been applied to distinguish intracellular and extracellular sodium, and to investigate macromolecule-bound environments of sodium (Pekar et al., 1987; Eliav and Navon, 1994; Navon et al., 1994; Knubovets et al., 1994; Shinar et al., 1993, 1994; Rooney and Springer, 1991a; Hutchison et al., 1990; Eliav et al., 1992; Kemp-Harper and Wimperis, 1993; Reddy et al., 1995; Whang et al., 1994; Furo et al., 1993; Tauskela and

Received for publication 2 June 1995 and in final form 1 November 1995.
Address reprint requests to Dr. Scott D. Kennedy, Department of Biophysics, University of Rochester Medical Center, 601 Elmwood Ave., Rochester, NY 14642. Tel.: 716-275-7585; Fax: 716-275-6007; E-mail: sdkenn@biophysics.rochester.edu.

0006-3495/96/02/715/00 $2.00

Shoubridge, 1993). Double-quantum coherence (DQC) can occur in quadruploar nuclei with spin 3/2 by two distinct mechanisms (Jaccard et al., 1986). First, if the relaxation rates of the satellite and central transitions are not equal, then density matrix operators of rank 3 will contribute to the generation of DQC. Second, if anisotropic modulation of the quadrupolar interaction tensor results in nonvanishing quadrupolar couplings, then density matrix operators of rank 2 will also contribute to the generation of DQC. In this work, we report ^{35}Cl DQF signals that are caused specifically by the band 3 anion transport site in intact red blood cells. We demonstrate that ^{35}Cl DQF NMR or multiple-exponential analyses can be used to distinguish transport site binding without the need for parallel experiments with inhibitors present. These results represent the first observation of DQF NMR signals from ^{35}Cl.

MATERIALS AND METHODS

Reagents

EM (eosin-5-maleimide) was purchased from Molecular Probes (Eugene, OR) and DNDS (4,4′-dinitrostilbene-2,2′-disulfonate) was from ICN Pharmaceuticals (Plainview, NY). EM and DNDS were made up as 1 mM and 2 mM stocks, respectively, in the 150 KH buffer (see below). All experiments with EM and DNDS as inhibitors were carried out in semidarkness because those two chemicals are light sensitive. The dissolved DNDS was always used within 2 days. Some of the EM stocks were kept for longer periods at −20°C.

Cell preparation and inhibitor treatment

Red blood cells were obtained from freshly drawn blood, donated by apparently healthy volunteers. Heparin was added as anticoagulant. The cells were washed at least 3 times with 150 KH (150 mM KCl, 24 mM sucrose, 20 mM HEPES, 5 mM glucose, pH 6.9, at room temperature). For each wash, the cells were centrifuged, the resulting supernatant and buffy coat were removed by aspiration, and then the cells were resuspended. The cells were then subjected to different treatments as described below. The cells were stored on ice before NMR measurement. Most of the measurements were completed within 36 h after the blood had been drawn.

To achieve nearly complete binding of band 3 with DNDS, enough DNDS was added to the samples to achieve more than 98% inhibition of Cl^- exchange. Based on the measurement that ID_{50} for DNDS is 4.11 μM in 150 mM Cl^- medium (Knauf et al., 1993b), the final concentration of DNDS in the sample was at least 400 μM (based on total sample volume).

The treatment with EM was carried out in the dark at 37°C in 150 KH buffer (pH = 6.71). To obtain more than 99% inhibition of Cl^- exchange, the cells were treated with 300 μM EM in 150 KH at 10% hematocrit for 2 h (Liu and Knauf, 1993).

^{35}Cl NMR

NMR data were taken with a 9.4 Tesla Bruker/GE (Fremont, CA) Omega NMR spectrometer operating at a frequency of 39.2 MHz for ^{35}Cl (400 MHz for protons). A 10-mm-diameter broad-band tunable probe was used. Acquisition parameters are given in the figure legends. Temperature of the sample was controlled by flow of regulated air. Magnetic field homogeneity was adjusted on the water proton resonance of a buffer sample, and proton linewidths of 3–5 Hz were typically obtained. Proton linewidths of cell suspensions were typically 12–15 Hz. Thus, distortions of the magnetic field even in samples containing red cells have minor effects on the decay of ^{35}Cl transverse magnetization.

^{35}Cl DQF signals were generated with the pulse sequence (Bax et al., 1980; Jaccard et al., 1986):

$$90° - \tau/2 - 180° - \tau/2 - \beta° - \delta - \beta° - \text{Acq.}$$

where τ is the creation time and δ is a 2-μs delay to reset the radio frequency phase. The pulse and receiver phase cycling scheme is that given by Bax et al. (Bax et al., 1980). The flip angle β is 90° when detection of rank 2 and 3 interactions is desired, and β is 54.7° when detection of only rank 2 interactions is desired (Jaccard et al., 1986; Eliav and Navon, 1994).

Data analysis

The NMR data were processed with the spectrometer software. Before mono- or multiexponential analyses, the effect of off-resonance signals was eliminated by calculating the magnitude of each point in the FID. The program CONTIN used for calculating T_2 distributions was obtained from Prof. S. W. Provencher (1982a,b). Forty points were used in the relaxation time grid. Biexponential analysis of the intracellular signal was performed by first fitting the extracellular signal and subtracting the calculated fit from data in Fig. 1.

RESULTS

Signal from intracellular ^{35}Cl can be excluded

The free induction decay of the ^{35}Cl NMR signal of a buffer solution containing 150 mM sodium chloride is shown in Fig. 1 along with the signal obtained when RBCs are present. The signal from ^{35}Cl in the absence of RBCs is well characterized as an exponential function with a T_2 of 19.9 ms at 10°C. In the presence of RBCs (50% hematocrit), a rapidly decaying component is clearly identified with decay time constant of approximately 400 μs when treated as a single component, and decay time constants of ~130 μs and ~700 μs when treated as biexponential. This component arises from ^{35}Cl inside the cells, where there is a high

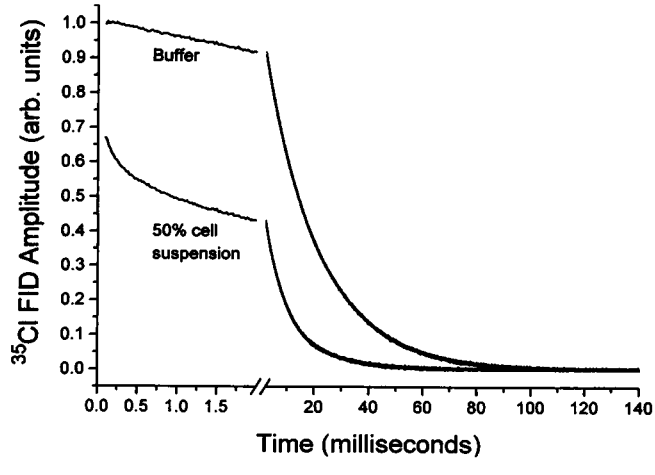

FIGURE 1 ^{35}Cl NMR signal (magnitude display) of a sample containing standard buffer (150 mM KCl) and a sample with red blood cells (50% hematocrit) suspended in standard buffer. 20,000 scans were averaged with sweep width equal to 50,000 Hz, and 8,192 complex data points were acquired in each scan. Much of the intracellular signal could not be observed because of the 115 μs receiver dead time, which is dominated by probe recovery time.

concentration of hemoglobin, whereas the more slowly decaying signal ($T_2 \approx 7$ ms) arises from extracellular ^{35}Cl. Riddell and Zhou (1995) have applied a relaxation agent to observe the intracellular ^{35}Cl signal and report similar time constants. Thus, separation of intracellular and extracellular ^{35}Cl signals is easily accomplished by delaying the start of signal acquisition for approximately 1–1.5 ms after the excitation pulse. This feature has been exploited by Falke et al. (1984a). Henceforth, all data and discussion refer only to the extracellular signal.

There are two components for control cell FID

When the extracellular ^{35}Cl signal obtained from a control cell suspension (no DNDS added) was fitted to a single exponential function, a systematic deviation was observed. This is very clearly seen from the residual plot (Fig. 2 *b*). If differences between the relaxation rates for the central and satellite transitions of ^{35}Cl are responsible for this behavior, it should be possible to fit the FID data with a function containing two exponential terms, with the faster and slower components having amplitudes in the ratio of 3:2. Indeed, Fig. 2 *c* shows that when the data are fitted to such a function the residuals are reduced to less than 0.75% of the initial signal amplitude. In contrast, the signals from buffer and DNDS-treated cells are well characterized by an exponential function (Fig. 2, *e* and *g*). T_2 in DNDS-treated cell suspensions is equal to T_2 of the slowly decaying signal of control suspensions (T_{2s}).

To test the hypothesis that control samples exhibit biexponential relaxation, whereas buffer or DNDS-treated samples do not, by a method that does not presume a particular physical model for the relaxation process, we used the CONTIN algorithm developed by Provencher (1982a). This program performs an analysis that approximates an inverse Laplace transform to describe data as the sum of a nearly continuous series of exponential functions, i.e., $f(t) = \sum_{i=1}^{n} A_i \exp(t/T_{2i})$. The solutions are constrained by the physically reasonable assumption that the relaxation times are not negative, and the relaxation time distribution (A_i) is required to be smooth. This algorithm has been employed in a variety of other NMR studies (Springer et al., 1994; Hinton and Johnson, 1993; Morris and Johnson, 1993; Lee et al., 1993; Hills and Babonneau, 1994). When applied to ^{35}Cl FIDs, relaxation time distributions for buffer and DNDS-treated cells show a single peak, whereas the distribution for a control cell suspension shows one additional peak (Fig. 3).

The results of the CONTIN analysis confirm the presence of two exponential decay components in control, but not in DNDS-treated cells. The small difference between the position of the T_2 peak for DNDS-treated cells and the slow T_2 peak for control cells is likely an artifact of the CONTIN analysis, which does not include the physically required constraint that the amplitudes of the fast and slow components have a 3:2 ratio. No such difference is observed in the fits in Fig. 2. Even if there is a small difference in T_2 for these two decays as a result of relaxation due to a DNDS/Cl^-/band 3 complex, the effects of DNDS still provide evidence that the additional relaxation component in control cells results from Cl^- binding to band 3 in its native state (without DNDS bound).

^{35}Cl DQF signal is caused by binding of Cl^- to the external transport site

If one of the decay components of the extracellular ^{35}Cl signal in RBC suspensions arises from the central transition of the spin system, whereas the other component arises from

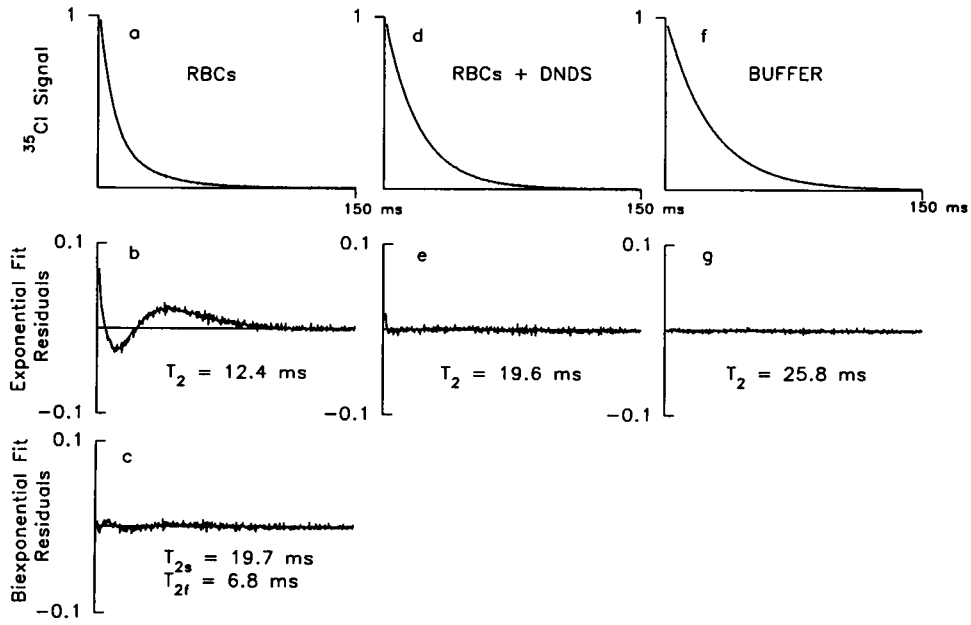

FIGURE 2 The magnitude of ^{35}Cl free induction decay signals from (*a*) a red blood cell suspension (50% hematocrit), (*d*) a red blood cell suspension with DNDS added, and (*f*) buffer used for the suspensions. (*b*, *e*, and *g*) The residuals after fitting the data in *a*, *d*, and *f*, respectively, to an exponential function. (*c*) The residuals after fitting the data in *a* to the function $y = 0.4 \exp(-t/T_{2s}) + 0.6 \exp(-t/T_{2f})$. The time constants derived from these analyses are listed on the residual plots. The first point in each data set was acquired 1.39 ms after the 90° pulse. A small (<2%) signal contribution from intracellular ^{35}Cl in RBC samples is detected in the first 1–2 points of the residual plots. The sweep width is 3300 Hz, 512 complex data points were acquired in each scan, and 6000 scans were averaged.

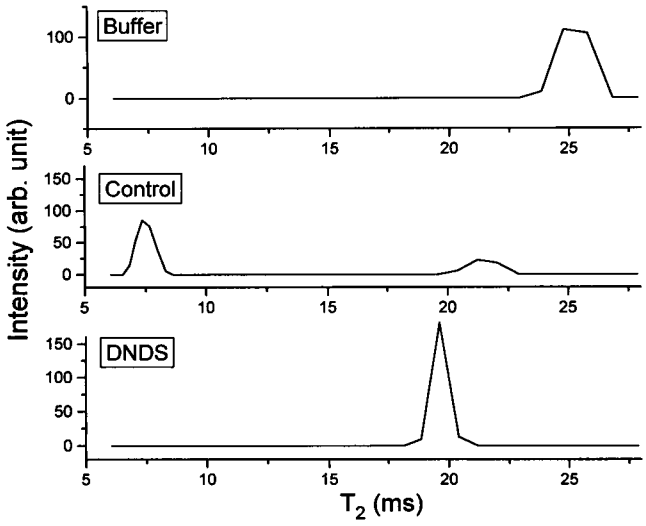

FIGURE 3 The T_2 distributions for buffer, control cells, and DNDS-treated cells calculated with the program CONTIN using the data shown in Fig. 2.

the satellite transitions, then double-quantum coherence can be created (Jaccard et al., 1986; Rooney and Springer, 1991b). DQF NMR was applied to buffer, DNDS-treated cells, and control cells (Fig. 4). The creation time (τ_c) was varied from 0.5 ms to 100 ms. Only control cells gave an observable double quantum signal, and the most intense signal appeared at τ_c = 15 ms. Although DNDS-treated cells exhibit a significant line-broadening relative to buffer because of nonspecific sites, no DQF signal is observed. The absence of a double-quantum signal with DNDS present indicates that only Cl^- binding to the transport sites can give rise to a DQF signal.

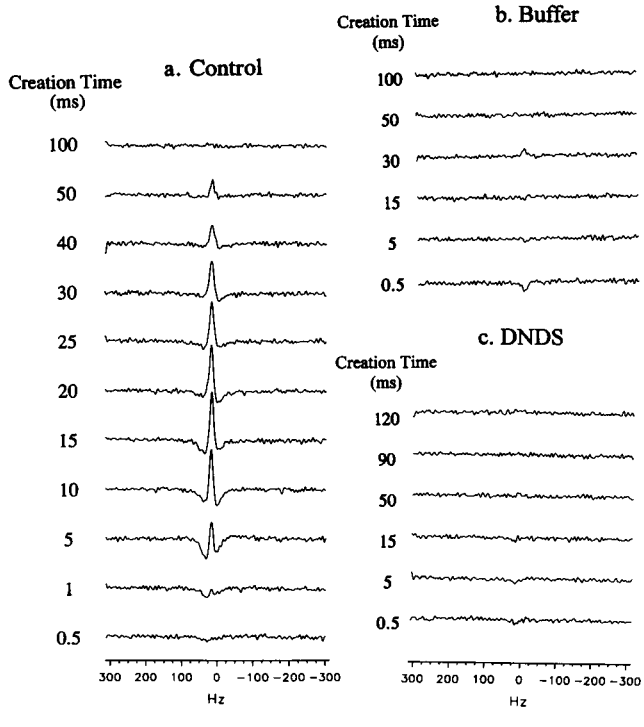

FIGURE 4 Double-quantum-filtered ^{35}Cl NMR spectra (β = 90°) of (*a*) red blood cell suspension, (*b*) buffer used for the suspensions (see Materials and Methods), and (*c*) red blood cell suspension with DNDS added. The creation time (τ) is listed with each spectrum. The sweep width is 2000 Hz, 256 complex data points were acquired in each scan, and 4800 scans were averaged.

The inhibitor EM does not block access to the chloride-binding site

Besides DNDS, another anion exchange inhibitor, EM, was also used to treat the cells. Flux experiments have shown that EM labeling inhibits more than 99% of Cl^- exchange under the conditions of our experiments (Liu and Knauf, 1993). Nevertheless, EM-treated cells still give a DQF signal (Fig. 5). This result supports the hypothesis that EM does not block anion access to the external facing site, but instead inhibits chloride flux by preventing translocation of ions once they are bound at the transport site (Liu et al., 1995).

Residual quadrupolar coupling contributes to DNDS-sensitive DQF signal

It has been shown that by setting the flip angle β equal to 54.7° instead of 90°, the contributions to the DQF signal from rank 3 interactions are eliminated and double-quantum coherence is due only to operators of rank 2, which are nonzero only if anisotropic motion results in nonvanishing quadrupolar couplings (Jaccard et al., 1986). We performed this experiment on control cell suspensions. The result (Fig.

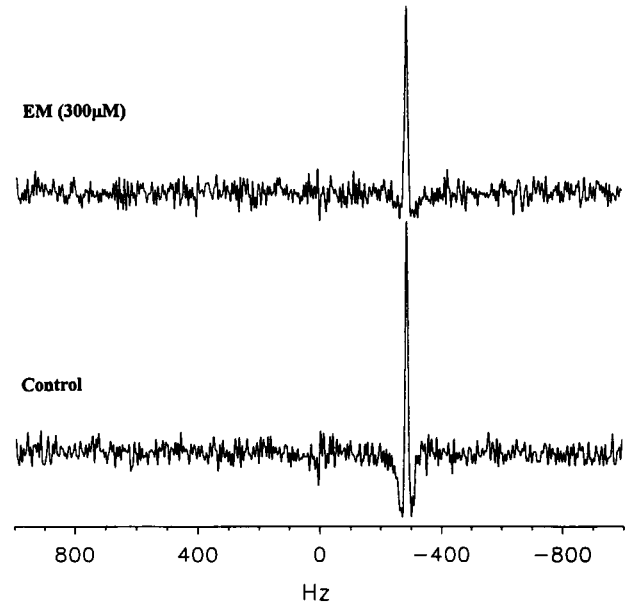

FIGURE 5 The DQF ^{35}Cl NMR spectra of control and EM-treated cell suspensions. The creation time was 15 ms, where the signal amplitude is the largest for control cells. Other acquisition parameters are the same as in Fig. 4.

6, *a* and *b*) shows that a large DQF signal remains when $\beta = 54.7°$, indicating that there is a significant contribution to the DQF signal from terms of rank 2. Fig. 6 *c* shows a simulation of the data in Fig. 6 *b* using the analysis of Eliav and Navon (1994), which is discussed in more detail later (Eqs. 6 and 7). The parameters used in the simulation were selected by fitting the peak heights in Fig. 6 *b* to Eq. 6 ($\omega = 0$) with the residual quadrupolar coupling constant ($P_B\bar{\omega}_{Q1}$) and the intrinsic relaxation rate of the rapidly decaying component (d_1) as adjustable parameters.

DISCUSSION

The transport of chloride across RBC membranes has been extensively studied (Jennings, 1992). The half-time for Cl^- exchange in dilute RBC suspensions is 454 ms at 20°C and increases to 17.2 s at 0°C (Brahm, 1977). At 50% hematocrit the half-times are a factor of 2 shorter. This means that intracellular and extracellular chloride populations do not mix during the approximately 400-μs half-life of the intracellular ^{35}Cl signal, and the signals from the two populations are separately observed in Fig. 1.

The decay of the signal from the extracellular ^{35}Cl population is not adequately described by a mono-exponential function unless the chloride binding site of band 3 is blocked (Figs. 2 and 3). Nonexponential magnetization decay of a spin 3/2 nucleus such as ^{35}Cl is observed when signals from the central transition and the satellite transitions have different relaxation properties. Both homogeneous and inhomogeneous broadening mechanisms may contribute to the decay rates. The homogeneous contribution to the transverse magnetization relaxation of spin 3/2 nuclei exchanging between a dilute, macromolecule bound environment (B) and aqueous solution (F) is approximated by (Swift and Connick, 1962; Bull, 1972; Falke et al., 1984b)

$$M_x(t) = M(0)\{(3/5)e^{-d_1 t} + (2/5)e^{-d_2 t}\} \quad (1)$$

where

$$d_i = s_{Fi} + \frac{P_B}{\tau_B}\left\{\frac{s_{Bi}(s_{Bi} + \tau_B^{-1}) + \Delta\omega_i^2}{(s_{Bi} + \tau_B^{-1})^2 + \Delta\omega_i^2}\right\}, \quad (2)$$

with $i = 1$ for the satellite transition and $i = 2$ for the central transition. P_B is the fraction of Cl^- in the bound state and is assumed to be much less than 1, and τ_B is the lifetime of Cl^- in the bound state. s_{Fi} and s_{Bi} are the intrinsic spin-spin relaxation rates s_i ($i = 1, 2$) in the free and bound environments, respectively, where (assuming a single time correlation function)

$$s_1 = C_Q^2\left[\tau_c + \frac{\tau_c}{(1 + \omega_o^2\tau_c^2)}\right] \quad (3)$$

and

$$s_2 = C_Q^2\left[\frac{\tau_c}{(1 + \omega_o^2\tau_c^2)} + \frac{\tau_c}{(1 + 4\omega_o^2\tau_c^2)}\right] \quad (4)$$

s_1 and s_2 are the satellite and central transition spin-spin relaxation rates, respectively, τ_c is the correlation time describing the modulation of the electric quadrupolar interaction, C_Q is the strength of the interaction fluctuations, and ω_o is the Larmor frequency. Note that $s_1 \geq s_2$, so the relaxation rate of the satellite transition is greater than or equal to that for the central transition. Also, if $\omega_o\tau_c \gg 1$,

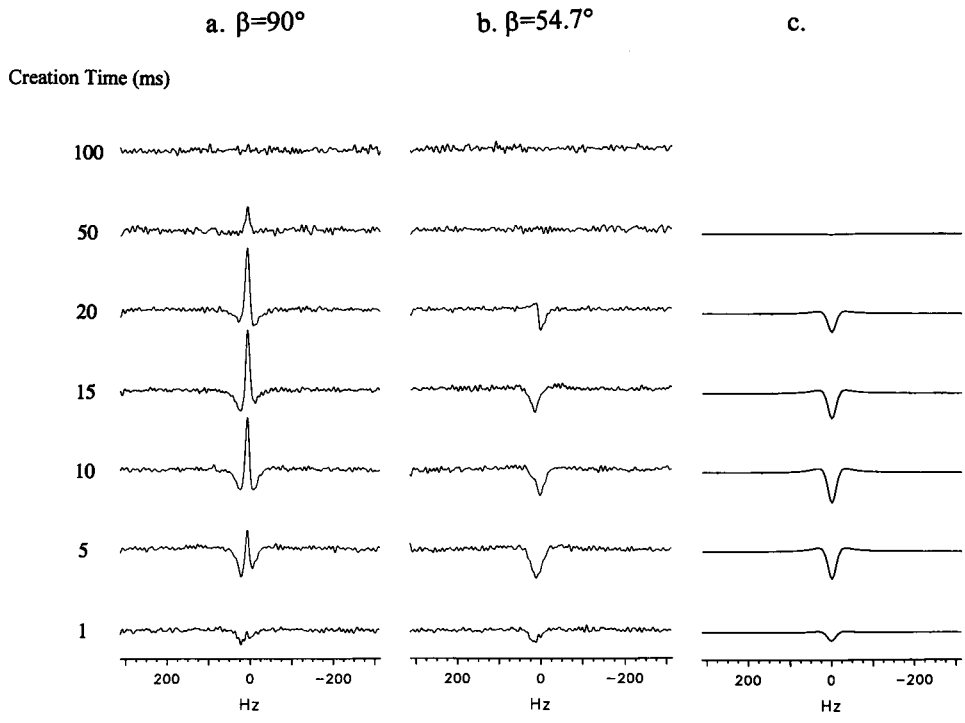

FIGURE 6 Double-quantum-filtered ^{35}Cl NMR spectra of a red blood cell suspension with (*a*) flip angle $\beta = 90°$ and (*b*) $\beta = 54.7°$. The creation time (τ) is listed with each spectrum. Other acquisition parameters are the same as in Fig. 4. (*c*) DQ spectra ($\beta = 54.7°$) calculated using Eqs. 6 and 7 with $P_B\bar{\omega}_{Q1}/2\pi = 15 \pm 3.5$ Hz and $R_{2f} = 104 \pm 16$ s^{-1}. The parameters were selected by fitting the peak heights in *b* to Eq. 6 ($\omega = 0$) with $P_B\bar{\omega}_{Q1}$, R_{2f}, and amplitude (A) as adjustable parameters.

$s_2 \rightarrow 0$ and the relaxation rate of the central transition is unaffected by the quadrupolar interaction. $\Delta\omega_i$ ($i = 1, 2$) is the change in resonance frequency of a transition upon binding to the macromolecule, which is caused by a nonzero first-order quadrupolar interaction:

$$\Delta\omega_i = \bar{\omega}_{Qi}(3\cos^2\theta_L - 1), \quad (5)$$

where $\bar{\omega}_{Qi}$ is the residual, bound-state quadrupolar coupling constant after partial averaging by rapid, anisotropic motion, and θ_L is the angle between the principal axis of the residual quadrupolar coupling tensor and the magnetic field. The central transition is affected by the residual quadrupolar coupling only to second order, so $\bar{\omega}_{Q2} \ll \bar{\omega}_{Q1}$. Although chemical shift may also contribute to $\Delta\omega_i$, it is neglected here because the chemical shift of the solution ^{35}Cl signal is unaffected by the presence of red blood cells. Finally, because the binding sites are randomly oriented, Eq. 1 must also include an integral over θ_L.

If $\bar{\omega}_{Q1} \neq 0$, the spectrum of the satellite transition signals will also have inhomogeneous broadening contributions with width given approximately by $P_B\bar{\omega}_{Q1}$, whereas the central transition remains unchanged to first order. However, the "powder pattern" collapses if a chloride ion binds to many sites with random orientations in a time τ_M that is short compared to ${\bar{\omega}_{Q1}}^{-1}$. The biexponential nature of Eq. 1 does not describe inhomogeneous broadening. In particular, the presence of inhomogeneous broadening could account for the small residuals seen for the biexponential fit in Fig. 2 *c*. Nonetheless, the qualitative aspects of Eqs. 1–5 are still very useful.

The exponential ^{35}Cl signal obtained from buffer demonstrates that $s_{F1} = s_{F2}$ (i.e., $\omega_o\tau_c \ll 1$) and that there is no residual quadrupolar coupling as expected. In the presence of RBCs treated with DNDS, the ^{35}Cl signal is still described by an exponential function, although the associated T_2 value is decreased relative to T_2 in the buffer. Reference to the above discussion of Eqs. 1–5 shows that nonnegligible bound-state relaxation can only be exponential (i.e., $d_1 = d_2$) if a) relaxation of both transitions is exchange limited (${\tau_B}^{-1} \ll s_{B2}$ and s_{B1}, or ${\tau_B}^{-1} \ll \bar{\omega}_{Q2}$ and $\bar{\omega}_{Q1}$), or b) extreme narrowing conditions apply ($s_{B1} = s_{B2}$) and the quadrupolar coupling vanishes ($\bar{\omega}_{Q1} = 0$). ^{37}Cl and ^{35}Cl NMR measurements as a function of temperature by Price et al. (1991), Falke et al. (1985b), and ourselves (data not shown) demonstrate that DNDS-insensitive line broadening is not limited by the rate of Cl^- binding and release. Thus, chloride ion dynamics at binding sites in DNDS-treated cell suspensions, where mono-exponential functions describe the NMR data very well, are in the extreme narrowing regime. Although we must also conclude that $\bar{\omega}_{Q1}$ vanishes, the NMR experiments do not allow any distinction between averaging of the quadrupolar coupling by isotropic motions within the binding sites and averaging by rapid exchange (${\tau_M}^{-1} \gg \bar{\omega}_{Q1}$) among sites of random orientation. The latter case might represent a reasonable model for nonspecific, largely electrostatically driven interactions with groups on the membrane surface. In addition, assuming a diffusion coefficient 1×10^{-5} cm^2/s, chloride ions can diffuse 4.5 μm within 10 ms. Thus some averaging of the quadrupolar tensor may result from diffusion of Cl^- around the edges of the cell or to other cells.

The nonexponential ^{35}Cl signal obtained from control cell suspensions suggests the presence of a site for which $s_1 \neq s_2$ (nonextreme narrowing) or $\bar{\omega}_{Q1} \neq 0$, or both, resulting in nonequivalence of d_1 and d_2. However, it is also possible that the nonexponential signal could arise from the superposition of signals from microdomains that do not mix. Jaccard et al. (1986) have demonstrated that, under conditions of nonextreme narrowing or nonvanishing quadrupolar couplings, multiple quantum (MQ) coherences can be created through the application of further pulses, and MQ filters can be applied to detect the presence of those coherences. If the nonexponential signal is due to microdomains that do not mix, no MQ signal is observed. The data in Fig. 4 demonstrate that ^{35}Cl DQC is readily created in control cell suspensions, indicating the presence of a site where chloride ion motions are either anisotropic ($\bar{\omega}_{Q1} \neq 0$) or in the nonextreme narrowing regime ($s_1 \neq s_2$), or both.

The DQF signal is eliminated and the nonexponential signal reverts to an exponential form upon addition of DNDS, which interferes with Cl^- binding to the transport site (Fröhlich, 1982). This result strongly suggests that the transport site of band 3 causes the DQF signal and nonexponential magnetization decay. Therefore, the data demonstrate that the chloride-binding site on the anion transporter band 3 is the only site on the extracellular surface of a red blood cell that substantially inhibits the motions of the chloride ion and is present in sufficient quantity to be detected by NMR.

Previous studies (Liu et al., 1995; Falke et al., 1984b) have demonstrated that the line broadening in DNDS-treated cells is approximately equal to the nonsaturable (low-affinity) line broadening of control cells. The data in Figs. 2 and 3 show that the ^{35}Cl T_2 value in DNDS-treated cell suspensions is approximately equal to T_{2s} (T_2 of central transition) in control cells at subsaturating Cl^- concentrations. Thus, the band 3 binding site does not appear to alter the relaxation rate of the central transition (s_2 from Eq. 4), which indicates $\omega_o\tau_c \gg 1$ in this site. This is further supported by the observation that ^{35}Cl spin-lattice relaxation, T_1, is the same in control and DNDS-treated cell suspensions (data not shown). Like s_2, the contribution to $1/T_1$ from a binding site is zero if $\omega_o\tau_c \gg 1$ for that site (Bull, 1972).

Price et al. (1991) have observed nonexponential ^{37}Cl and ^{35}Cl relaxation in red blood cell ghost preparations. In contrast to our observation, they observe that the nonexponential character is not completely removed by the addition of DNDS. This result may be due to Cl^- sites on the inner surface of the membrane that are not accessible in intact cell suspensions.

Previous ^{35}Cl NMR studies of anion transport inhibitor mechanisms detected Cl^- binding to the transport site by calculating the difference between linewidths from RBC or ghost suspensions containing the inhibitor of interest and

samples containing DNDS (Falke and Chan, 1986a,b,c; Liu et al., 1995). A problem with this method is that the difference may represent a small fraction of the total line broadening, or that the inhibitor and DNDS may interact, making it impossible to use DNDS to identify the transport site line broadening. The results presented in this work suggest that DQF experiments or multiexponential analyses will detect transport site binding without the need for a reference sample with DNDS (or other previously characterized inhibitors). For example, we have previously reported that the binding of the inhibitor EM does not block the access of Cl^- to the transport sites, regardless of whether EM is reversibly (Knauf et al., 1993b) or covalently (Liu et al., 1995) bound. The observation of a DQF signal from EM-labeled cells provides further evidence for this conclusion.

The DQF signal can have contributions from rank 2 and rank 3 interactions. Rank 2 interactions contribute only in the presence of residual quadrupolar couplings ($\bar{\omega}_{Q1} \neq 0$). Rank 3 interactions contribute to DQC if motional processes are in the nonextreme narrowing regime ($\omega_o\tau_c \geq 1$), and can also contribute if $\bar{\omega}_{Q1} \neq 0$ (Eliav and Navon, 1994). Eliav et al. have presented detailed analyses of DQF signals from ^{23}Na (Eliav and Navon, 1994; Shinar et al., 1993, 1994; Knubovets et al., 1994) filtered to retain only rank 2 contributions. Whereas setting $\beta = 54.7°$ completely removes DQ coherence due to terms of rank 3, contributions from terms of rank 2 are only multiplied by a factor of 0.67 relative to the signal obtained when $\beta = 90°$ (Eliav and Navon, 1994; Shinar et al., 1993). Thus, the data in Fig. 6, *a* and *b*, demonstrate that motion of Cl^- in the transport site anisotropically reorients the quadrupolar interaction tensor, which results in a substantial contribution to the total DQF signal. The residual quadrupolar coupling in the bound environment ($\bar{\omega}_{Q1}$) can be estimated by comparing the analysis of Eliav and Navon (1994) to the data in Fig. 6 *b* if the concentration of binding sites (P_B) is known and the exchange rate between free and bound is assumed to be much greater than $\bar{\omega}_{Q1}$. In this case, the DQ-filtered spectrum for $\beta = 54.7°$ is given by

$$F(\tau, \omega) = \int_0^{\pi/2} A \sin(P_B\Delta\omega_1\tau)e^{-\tau R_{2f}}g(\omega)\sin(\theta_L)\, d\theta_L \qquad (6)$$

and

$$g(\omega) = \frac{P_B\Delta\omega_1 + \omega}{R_{2f}^2 + (P_B\Delta\omega_1 + \omega)^2} + \frac{P_B\Delta\omega_1 - \omega}{R_{2f}^2 + (P_B\Delta\omega_1 - \omega)^2} \qquad (7)$$

where $\Delta\omega_1$ is given in Eq. 5, and R_{2f} is the spin-spin relaxation rate of the satellite transition. The spectra in Fig. 6 *c* were calculated using Eqs. 6 and 7. The rise of the signal at short creation times is determined by the integral over θ_L of the quantity $\sin[P_B\bar{\omega}_{Q1}(3\cos^2\theta_L - 1)\tau]$ in Eq. 6, and the value of $P_B\bar{\omega}_{Q1}$ must be the same order of magnitude as R_{2f} if a signal is observed. The ratio $(P_B\bar{\omega}_{Q1})/R_{2f} = 0.91$ for the parameters used in calculating the spectra in Fig. 6 *c*. Because the concentration of band 3 in the red blood cell suspensions (50% hematocrit) is approximately 16.6 μM (Wieth and Bjerrum, 1983) and the Cl^- concentration is 150 mM, $P_B \approx 10^{-4}$ if all sites are assumed to be filled and facing outward. Therefore, from the value of $P_B\bar{\omega}_{Q1}/2\pi = 15$ Hz, the residual quadrupolar coupling constant, $\bar{\omega}_{Q1}/2\pi$, is approximately 135 kHz for ^{35}Cl bound in the transport site of band 3. This value may be an underestimate because the assumption of rapid exchange may not be appropriate (Liu et al., 1995; Falke et al., 1985b; Price et al., 1991), and because most of the sites may face inward.

In the above analysis, no attempt is made to model contributions of rank 3 interactions to the DQF signal when $\beta = 90°$. These interactions may include contributions from slow motions if $\tau_c \geq 1/\omega_o \approx 4$ ns. Contributions from rank 3 terms are indicated by the observation of a nonzero triple-quantum-filtered signal (data not shown). Furthermore, the DNDS insensitivity of the central transition relaxation rate (as discussed above) implies $\tau_c \gg 1/\omega_o$ for chloride bound in the band 3 transport site.

CONCLUSION

The NMR signal of extracellular ^{35}Cl in red blood cell suspensions is observed to decay nonexponentially. The signal returns to an exponential form when DNDS is added. Similarly, the double-quantum-filtered ^{35}Cl signal from the same suspensions is eliminated in the presence of DNDS. These data demonstrate that the chloride-binding site on the anion transporter band 3 is the only NMR observable site on the extracellular surface of a red blood cell that substantially inhibits the motions of the ion. Anisotropic reorientation of the ^{35}Cl quadrupolar interaction tensor in the band 3 transport site is indicated by a large rank 2 filtered DQF signal. The DQF signal in the presence of the anion transport inhibitor EM provides further evidence that EM does not block access to the transport site.

Dr. Denise Hinton is gratefully acknowledged for her assistance with the CONTIN algorithm. Helpful discussions with Dr. R. G. Bryant are gratefully acknowledged.

Supported by NIDDK grant DK27495 National Cancer Institute grant CA11198.

REFERENCES

Aranibar, N., C. Ostermeier, B. Legrum, H. Rüterjans, and H. Passow. 1994. Influence of stilbene disulfonates on the accessibility of the substrate-binding site for anions in the band 3 protein (AEB1). *Ren. Physiol. Biochem.* 17:187–189.

Bax, A., R. Freeman, and S. P. Kempsell. 1980. Natural abundance ^{13}C-^{13}C coupling observed via double-quantum coherence. *J. Am. Chem. Soc.* 102:4849–4851.

Brahm, J. 1977. Temperature-dependent changes of chloride transport kinetics in human red cells. *J. Gen. Physiol.* 70:283–306.

Bull, T. E. 1972. Nuclear magnetic relaxation of spin-3/2 nuclei involved in chemical exchange. *J. Magn. Reson.* 8:344–353.

Eliav, U., and G. Navon. 1994. Analysis of double-quantum-filtered NMR spectra of ^{23}Na in biological tissues. *J. Magn. Reson. B.* 103:19–29.

Eliav, U., H. Shinar, and G. Navon. 1992. The formation of a second-rank tensor in ^{23}Na double-quantum-filtered NMR as an indicator for order in a biological tissue. *J. Magn. Reson.* 98:223–229.

Falke, J. J., and S. I. Chan. 1985. Evidence that anion transport by band 3 proceeds via a ping-pong mechanism involving a single transport site: a ^{35}Cl NMR study. *J. Biol. Chem.* 260:9537–9544.

Falke, J. J., and S. I. Chan. 1986a. Molecular mechanisms of band 3 inhibitors. 1. Transport site inhibitors. *Biochemistry.* 25:7888–7894.

Falke, J. J., and S. I. Chan. 1986b. Molecular mechanisms of band 3 inhibitors. 2. Channel blockers. *Biochemistry.* 25:7895–7898.

Falke, J. J., and S. I. Chan. 1986c. Molecular mechanisms of band 3 inhibitors. 3. Translocation inhibitors. *Biochemistry.* 25:7899–7906.

Falke, J. J., K. J. Kanes, and S. I. Chan. 1985a. The minimal structure containing the band 3 anion transport site: a ^{35}Cl NMR study. *J. Biol. Chem.* 260:13294–13303.

Falke, J. J., K. J. Kanes, and S. I. Chan. 1985b. The kinetic equation for the chloride transport cycle of band 3: a ^{35}Cl and ^{37}Cl NMR study. *J. Biol. Chem.* 260:9545–9551.

Falke, J. J., R. J. Pace, and S. I. Chan. 1984a. Direct observation of the transmembrane recruitment of band 3 transport sites by competitive inhibitors. *J. Biol. Chem.* 259:6481–6491.

Falke, J. J., R. J. Pace, and S. I. Chan. 1984b. Chloride binding to the anion transport binding sites of band 3: a ^{35}Cl NMR study. *J. Biol. Chem.* 259:6472–6480.

Forsen, S., and B. Lindman. 1981. Ion binding in biological systems as studied by NMR spectroscopy. *Methods Biochem. Anal.* 27:289–486.

Fröhlich, O. 1982. The external anion binding site of the human erythrocyte anion transporter: DNDS binding and competition with chloride. *J. Membr. Biol.* 65:111–123.

Furo, I., B. Halle, and P.-O. Quist. 1993. A new method for selective detection of "invisible" quadrupolar satellites in heterogeneous systems. *J. Magn. Reson. B.* 102:84–90.

Galanter, W. L., and R. J. Labotka. 1991. The binding of nitrate to the human anion exchange protein (AE1) studied with ^{14}N nuclear magnetic resonance. *Biochim. Biophys. Acta.* 1079:146–151.

Glibowicka, M., B. Winckler, N. Aranibar, M. Schuster, H. Hanssum, H. Rüterjans, and H. Passow. 1988. Temperature dependence of anion transport in the human red blood cell. *Biochim. Biophys. Acta.* 946:345–358.

Hills, B. P., and F. Babonneau. 1994. A quantitative study of water proton relaxation in packed beds of porous particles with varying water content. *Magn. Reson. Imaging.* 12:909–922.

Hinton, D. P., and C. S. Johnson, Jr. 1993. Diffusion ordered 2D NMR spectroscopy of phospholipid vesicles: determination of vesicle size distributions. *J. Phys. Chem.* 97:9064–9072.

Hubbard, P. S. 1969. Nonexponential relaxation of three-spin systems in nonspherical molecules. *J. Chem. Phys.* 51:1647–1651.

Hubbard, P. S. 1970. Nonexponential nuclear magnetic relaxation by quadrupole interactions. *J. Chem. Phys.* 53:985–987.

Hutchison, R. B., D. Malhotra, R. E. Hendrick, L. Chan, and J. I. Shapiro. 1990. Evaluation of the double-quantum filter for the measurement of intracellular sodium concentration. *J. Biol. Chem.* 265:15506–15510.

Jaccard, G., S. Wimperis, and G. Bodenhausen. 1986. Multiple-quantum NMR spectroscopy of S = 3/2 spins in isotropic phase: a new probe for multiexponential relaxation. *J. Chem. Phys.* 85:6282–6293.

Jennings, M. L. 1992. Cellular anion transport. *In* The Kidney: Physiology and Pathophysiology. D. W. Seldin and G. Giebisch, editors. Raven Press, New York. 113–145.

Kemp-Harper, R., and S. Wimperis. 1993. Detection of the interaction of sodium ions with ordered structures in biological systems. Use of the Jeener-Broekaert experiment. *J. Magn. Reson. B.* 102:326–331.

Knauf, P. A., E. A. Ries, L. A. Romanow, S. Bahar, and E. S. Szekeres. 1993a. DNDS does not act as a purely competitive inhibitor of red blood cell band 3-mediated anion exchange. *Biophys. J.* 64:A307. (Abstr.)

Knauf, P. A., N. M. Strong, J. Penikas, R. B. Wheeler, Jr., and S. J. Liu. 1993b. Eosin-5-maleimide inhibits red cell Cl^- exchange at a noncompetitive site that senses band 3 conformation. *Am. J. Physiol.* 264: C1144–C1154.

Knubovets, T., H. Shinar, U. Eliav, and G. Navon. 1994. Characterization of the sodium binding site at the membrane of mammalian red blood cells—a multiple quantum filtered NMR study. *Proc. Soc. Magn. Res. 2:* 1154. (Abstr.)

Lee, J.-H., C. Labadie, C. S. Springer, Jr., and G. S. Harbison. 1993. Two-dimensional inverse Laplace transform NMR: altered relaxation times allow detection of exchange correlation. *J. Am. Chem. Soc.* 115: 7761–7764.

Liu, D., S. D. Kennedy, and P. A. Knauf. 1995. ^{35}Cl NMR line-broadening shows that eosin-5-maleimide (EM) does not block the external anion access channel of band 3. *Biophys. J.* 69:399–408.

Liu, S. J., and P. A. Knauf. 1993. Lys-430, site of irreversible inhibition of band 3 Cl^- flux by eosin-5-maleimide, is not at the transport site. *Am. J. Physiol.* 264:C1155–C1164.

Minami, T., W. S. Price, and D. J. Cutler. 1992. Chloride-37 nuclear magnetic resonance spectroscopic study of binding of salicylic acid and other hydroxybenzoic acids to the band 3 anion transport protein of human erythrocytes. *J. Pharm. Sci.* 81:419–423.

Morris, K. F., and C. S. Johnson, Jr. 1993. Resolution of discrete and continuous molecular size distributions by means of diffusion-ordered 2D NMR spectroscopy. *J. Am. Chem. Soc.* 115:4291–4299.

Navon, G., J. G. Werrmann, R. Maron, and S. M. Cohen. 1994. ^{31}P NMR and triple quantum filtered ^{23}Na NMR studies of the effects of inhibition of Na^+/H^+ exchange on intracellular sodium and pH in working and ischemic hearts. *Magn. Reson. Med.* 32:556–564.

Pekar, J., P. F. Renshaw, and J. S. Leigh, Jr. 1987. Selective detection of intracellular sodium by coherence-transfer NMR. *J. Magn. Reson.* 72: 159–161.

Price, W. S., P. W. Kuchel, and B. A. Cornell. 1991. A ^{35}Cl and ^{37}Cl NMR study of chloride binding to the erythrocyte anion transport protein. *Biophys. Chem.* 40:329–337.

Provencher, S. W. 1982a. A constrained regularization method for inverting data represented by linear algebraic or integral equations. *Comput. Phys. Commun.* 27:213–227.

Provencher, S. W. 1982b. CONTIN: a general purpose constrained regularization program for inverting noisy linear algebraic and integral equations. *Comput. Phys. Commun.* 27:229–242.

Reddy, R., L. Bolinger, M. Shinnar, E. Noyszewski, and J. S. Leigh. 1995. Detection of residual quadrupolar interaction in human skeletal muscle and brain in vivo via multiple quantum filtered sodium NMR spectra. *Magn. Reson. Med.* 33:134–139.

Riddell, F. G., and Z. Zhou. 1995. NMR visibility of $^{35}Cl^-$ in human erythrocytes. *Magn. Reson. Chem.* 33:66–69.

Rooney, W. D., and C. S. Springer, Jr. 1991a. The molecular environment of intracellular sodium: ^{23}Na NMR relaxation. *NMR Biomed.* 4:227–245.

Rooney, W. D., and C. S. Springer, Jr. 1991b. A comprehensive approach to the analysis and interpretation of the resonances of spins 3/2 from living systems. *NMR Biomed.* 4:209–226.

Shinar, H., T. Knubovets, U. Eliav, and G. Navon. 1993. Sodium interaction with ordered structures in mammalian red blood cells detected by Na-23 double quantum NMR. *Biophys. J.* 64:1273–1279.

Shinar, H., T. Knubovets, Y. Sharf, U. Eliav, and G. Navon. 1994. The diversity of the residual quadrupolar interaction of Na-23 and H-2 in connective tissues evaluated by multiple quantum filtered NMR techniques. *Proc. Soc. Magn. Res.* 2:1152. (Abstr.)

Springer, C. S., Jr., C. Labadie, and J.-H. Lee. 1994. Relaxographic Imaging. *J. Magn. Reson. B.* 105:99.

Swift, T. J., and R. E. Connick. 1962. NMR-relaxation mechanisms of ^{17}O in aqueous solutions of paramagnetic cations and the lifetime of water molecules in the first coordination sphere. *J. Chem. Phys.* 37:307–320.

Tauskela, J. S., and E. A. Shoubridge. 1993. Response of the ^{23}Na-NMR double-quantum filtered signal to changes in Na^+ ion concentration in model biological solutions and human erythrocytes. *Biochim. Biophys. Acta.* 1158:155–165.

Whang, J., J. Katz, L. M. Boxt, K. Reagan, D. J. Sorce, R. R. Sciacca, and P. J. Cannon. 1994. Multiple-quantum-filtered NMR determination of equilibrium magnetization for ^{23}Na quantitation in model phantoms. *J. Magn. Reson. B.* 103:175–179.

Wieth, J. O., and P. J. Bjerrum. 1983. Transport and modifier sites in capnophorin, the anion transport protein of the erythrocyte membrane. *In* Structure and Function of Membrane Proteins. E. Quagliariello and F. Palmieri, editors. Elsevier Science Publishers B.V., Amsterdam. 95–106.